Plasmonics (2014) 9:1491–1500
DOI 10.1007/s11468-014-9768-2

Numerical study of nanoparticle sensors based on the detection of the two-photon-induced luminescence of gold nanorod antennas

Zaoshan Huang · Qiaofeng Dai · Sheng Lan · Shaolong Tie

Received: 2 May 2014 / Accepted: 6 August 2014 / Published online: 19 August 2014

Abstract We investigate numerically the modification of the nonlinear optical properties of a nanoantenna in the trapping of nanoparticles (NPs) by using both the discrete dipole approximation method and the finite-difference time-domain technique. The nanoantenna, which is formed by two gold nanorods (GNRs) aligned end to end and separated by a small gap, can emit strong two-photon-induced luminescence (TPL) under the excitation of a femtosecond laser light which is resonant with its longitudinal surface plasmon resonance. In addition, the excited antenna can stably trap small NPs which in turn induce modifications in the emitted TPL. These two features make it a promising candidate for building highly sensitive detectors for NPs of different materials and sizes. It is demonstrated that sensors built with antennas possess higher sensitivities than those built with single GNRs and nanorod-based antennas are more sensitive than nanoprism-based antennas. In addition, it is found that the trapping probability for a second NP is significantly reduced for the antenna with a trapped NP, implying that trapping of NPs may occur sequentially. A relationship between the TPL of the system (antenna+NP) and the optical potential energy of the NP is established, enabling the extraction of the information on the optical potential energy and optical force by recording the TPL of the system. It is shown that the sequential trapping and releasing of NPs flowing in a microfluid channel can be realized by designing two different antennas arranged closely.

Keywords Gold nanorod · Nanoantenna · Two-photon-induced luminescence · Optical potential energy · Optical force

Z. Huang · Q. Dai · S. Lan (✉)
Laboratory of Nanophotonic Functional Materials and Devices, School of Information and Optoelectronic Science and Engineering, South China Normal University, Guangzhou 510006, China
e-mail: slan@scnu.edu.cn

S. Tie
School of Chemistry and Environment, South China Normal University, Guangzhou 510006, China

Introduction

Localized surface plasmon polaritons (SPPs) or surface plasmon resonances (SPRs) excited in nanoparticles (NPs) of noble metals have been the focus of many studies due to their potential applications in various fields of nanometer science and technology [1]. Among metallic NPs of different shapes, gold nanorods (GNRs) have received intensive and extensive studies because of the chemical stability of gold and particularly the existence of longitudinal SPRs (LSPRs) which significantly modify the physical properties of GNRs [2]. A typical example in which the LSPRs of GNRs have been successfully utilized is the demonstration of five-dimensional optical data storage [3–5]. In this case, the strong polarization and wavelength dependences of LSPRs of GNRs were exploited to realize polarization and wavelength multiplexing in optical data storage.

It has been known that the LSPR of a GNR, which corresponds to the collective oscillations of electrons along the long axis of the GNR, exhibits a strong dependence on the dielectric environment surrounding the GNR [6]. This unique feature has been employed to fabricate sensors of different types [7–10]. The underlying physical mechanism is the existence of strongly localized electric field near the surface of the GNR. It has been demonstrated that the enhancement in local electric field near the surface of the GNR is so significant that the detection of the Raman scattering signal of single molecules becomes possible [11–13].

Basically, the optical properties of a GNR will be affected by an approaching NP through the modification of its LSPR. This property has been exploited to build sensors with different functions for NPs [8–10]. So far, the design of sensors or

detectors based on single GNRs generally relies on the detection of the modification in their linear optical properties such as scattering. From the experimental point of view, the LSPRs of GNRs can be detected through the measurements of the scattering spectra of GNRs by using dark-field microscopy [14–16]. However, the signal to noise ratio in the scattering spectra measurements is generally not satisfied for small GNRs whose extinction is dominated by absorption rather than scattering [17, 18]. On the other hand, the line width of the LSPRs of single GNRs, which reflects the homogeneous broadening of the LSPRs, is estimated to be ~100 meV at room temperature [15, 16]. For this reason, it is difficult to accurately determine the shift of LSPRs in most cases because of the broad line width. In practical applications, the difficulties in both the detection of LSPRs and the determination of their shift severely hinder the use of this property in making sensors with high sensitivities.

Very recently, a nanoear built with a gold NP trapped in a three-dimensional optical potential has been proposed to detect acoustic wave with ultrahigh sensitivity [19]. The principle of such a nanoear is to characterize the displacement of the trapped NP caused by the acoustic wave. The measurement of the displacement or distribution probability of the NP relies on the detection of the scattering light, offering a resolution of ~1.5 nm for the displacement. In practice, one can monitor the movement of nanoparticles much smaller than the diffraction limit by using dark-field microscopy. However, the determination of the sizes of NPs remains to be a challenge because it is difficult to establish a correlation between scattering light intensity and particle size.

Apart from their linear optical properties, the nonlinear optical properties of GNRs have become the focus of many studies in recent years [20–25]. Physically, it is anticipated that the detection of nonlinear optical properties, such as second harmonic generation (SHG) [20, 21] and two-photon-induced luminescence (TPL) [22, 23], will offer higher resolution in both the space and frequency domains. In experiments, SHG and TPL have been observed in GNRs of different sizes. Very recently, we demonstrated the existence of a size-dependent competition between SHG and TPL in GNRs [17]. In addition, we proposed the use of the TPL emitted by a single GNR to sense NPs approaching the GNR from far places [7]. From the viewpoint of practical application, however, the sensitivity and feasibility of the sensor need to be improved significantly. It has been demonstrated that a further enhancement in local electric field can be achieved in the narrow gap of a nanoantenna formed by two coupled GNRs which are arranged end to end [26, 27]. The coupling strength and the enhancement in local electric field depend strongly on the gap between the two GNRs. It is expected that the sensors made of such antennas would possess higher sensitivities than those made of single GNRs.

Another advantage of antennas over single GNRs is the well-defined optical potential well located at the narrow gap between the two constituent GNRs where NPs can be stably trapped [27, 28]. For the sensors based on single GNRs, the TPL of the system depends not only on the size of the NP but also on its position. Therefore, it is difficult to extract the information on the size of the NP without knowing the position of the NP [7]. In comparison, the stable trapping of NPs achieved in antennas makes it possible to estimate the sizes of NPs. Once a NP is trapped by an antenna, the SPR of the antenna would be significantly shifted [27, 28], leading to a dramatic reduction in the electric field intensity in the gap region. Consequently, the possibility of trapping another NP is greatly reduced until the trapped NP is released.

In this article, we propose a nanoantenna-based device capable of trapping and sensing NPs flowing in a microfluid channel. It is revealed by numerical calculation that the trapping possibility of another NP is reduced significantly once the antenna has trapped a NP. It is shown that antenna-based sensors possess higher sensitivities than those based on single GNRs and nanorod-based antennas are more sensitive than nanoprism-based antennas. The correlation between the TPL intensity of the system and the size of the trapped NP has been established if the material of the NP is known. By monitoring the evolution of the TPL of the system when the NP is approaching the antenna from a far place, it is possible to extract the profile for the optical potential energy of the NP and the optical force acting on the NP. The design of a practical device capable of sequentially trapping and releasing NPs is also proposed.

Physical Model and Numerical Method

The antenna-based device we proposed is schematically depicted in Fig. 1. In practice, it can be fabricated by three steps. First, an antenna composed of two coupled GNRs is fabricated on a substrate by using electron beam lithography and dry etching. Then, it is covered by a dielectric film such as a polymer film. Finally, a microfluid channel perpendicular to the long axis of the GNRs is built by using again lithography and etching. Its width (w) is smaller than the gap between the two GNRs (g), which is chosen to be g=6.0 nm in this work. NPs of different sizes and types can flow in the channel filled with water. The antenna is excited with a femtosecond (fs) laser light focused by using the objective of a microscope, and the excitation wavelength is resonant with the LSPR of the antenna (800 nm). The TPL emitted by the antenna is collected by using the same objective and directed to a detector (e.g., a PMT) connected to the microscope for analysis [17]. For simplicity, the refractive index of the polymer is assumed to be the same as that of water in the channel. In addition, we consider here nanospheres (NSs) made of Au, Si, and SiO_2

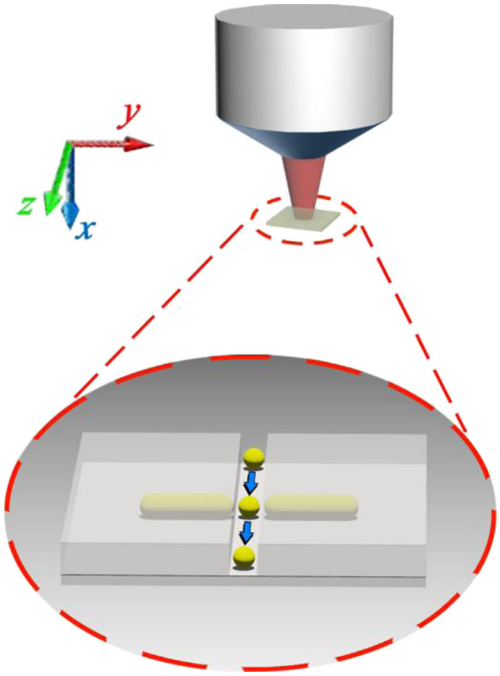

Fig. 1 Schematic showing the nanoantenna-based device capable of trapping and sensing NPs flowing in a microfluid channel through the detection of the TPL emitted by the system

with different diameters (ϕ) ranging from 3.0 to 5.0 nm. It should be emphasized that we chose to study GNRs, NSs, and microfluid channel with small sizes because of the limitation in computation source. In practice, the sizes of the GNRs, NSs, and microfluid channel can be scaled up without influencing most of the conclusions drawn in this work.

The two GNRs constituting the antenna are cigar-like GNRs composed of a cylinder and two hemispheres. The length and diameter of the GNRs are chosen to be l=22 and ϕ=6 nm, giving an aspect ratio of 3.67. Since the extinction of small GNRs is dominated by absorption [17, 18], we calculated the absorption spectra of single GNRs and the antenna by using the discrete dipole approximation (DDA) method [29, 30], as shown in Fig. 2. The dipole size was chosen to be 0.5 nm. It can be seen that the LSPR of the GNRs appears at ~775 nm while that of the antenna appears at 800 nm with enhanced absorption, implying a significant enhancement in local electric field. The absorption for the antenna shown in Fig. 2 is the linear absorption. In order to evaluate the TPL emitted by the antenna, one needs to consider the two-photon absorption (TPA) of the antenna excited by the fs laser light.

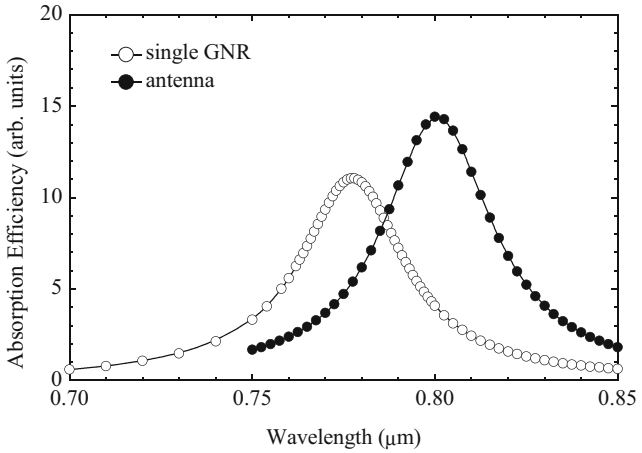

Fig. 2 Calculated absorption spectra for the antenna and the constituent GNRs

Very recently, we have established a numerical method to evaluate the TPL emitted by a single GNR [7] and the method can be easily extended to the calculation of the TPL emitted by an antenna. Basically, the TPL emitted by the system composed of an antenna and a NS can be expressed as follows [7]:

$$I_{\mathrm{TPL}}(x,y,z)\propto\eta|E_0|^4\int_{\mathrm{antenna}+\mathrm{NS}}|\mathbf{E}(\lambda_{\mathrm{ex}},x,y,z)/E_0|^4dV\cdot\int_{\mathrm{antenna}+\mathrm{NS}}|\mathbf{E}(\lambda_{\mathrm{em}},x,y,z)/E_0|^2dV \quad (1)$$

Here, η is the quantum efficiency of the GNRs, E_0 is the electric field of the incident light, and E(λ_{ex}, x, y, z) and E(λ_{em}, x, y, z) represent the electric fields inside the antenna and the NS at the excitation and emission wavelengths, respectively. The integration runs over the volume of the antenna and that of the NS.

Apparently, the TPL of the system depends on the position of the NS, which is represented by (x, y, z) in the coordinate shown in Fig. 1. If the origin of the coordinate is chosen at the gap center of the antenna, then the NS moving in the microfluid channel can be characterized by z only. When the antenna-based sensor is used to detect a NS, what we are concerned is the modification in the TPL intensity of the system (antenna+NS) rather than its absolute intensity. In other words, the TPL intensity of the system when the NS is far from the antenna (i.e., $z\rightarrow\infty$) can be used as reference for normalization.

$$I_{\mathrm{NOR}}=\frac{\int_{\mathrm{antenna}+\mathrm{NS}}|\mathbf{E}(\lambda_{\mathrm{ex}},x,y,z)/E_0|^4dV\cdot\int_{\mathrm{antenna}+\mathrm{NS}}|\mathbf{E}(\lambda_{\mathrm{em}},x,y,z)/E_0|^2dV}{\int_{\mathrm{antenna}+\mathrm{NS}}|\mathbf{E}(\lambda_{\mathrm{ex}},x,y,z\rightarrow\infty)/E_0|^4dV\cdot\int_{\mathrm{antenna}+\mathrm{NS}}|\mathbf{E}(\lambda_{\mathrm{em}},x,y,z\rightarrow\infty)/E_0|^2dV} \quad (2)$$

Since the TPL of the system (λ_{em}) appears mainly in the visible light region which is far from the LSPR of the antenna (λ_{ex}), the approaching of the NS does not change so much the electric field distribution at the emission wavelength (E(λ_{em}, x, y, z)). Therefore, its influence on the TPL can be neglected and I_{NOR} is further simplified as

$$I_{NOR} = \frac{\int_{\text{antenna + NS}} |\mathbf{E}(\lambda_{ex}, x, y, z)/E_0|^4 dV}{\int_{\text{antenna + NS}} |\mathbf{E}(\lambda_{ex}, x, y, z \to \infty)/E_0|^4 dV} \quad (3)$$

In addition to the evaluation of the TPL emitted by the system, we need to analyze the optical forces acting on the NSs flowing in the microfluid channel. In particular, it is important to know whether a NS can be stably trapped in the optical potential well formed in the gap of the antenna. For this reason, we employed the finite-difference time-domain (FDTD) technique [31, 32] to calculate the gradient forces acting on the NSs and derived the profiles for the optical potential wells created for different NSs. In our case, the optical force is dominated by the gradient force along the z direction. The y component of the optical force is negligible due to the symmetry of the structure and the x component of the optical force is three orders of magnitude smaller than the z component and will be balanced by the supporting force provided by the channel. In the FDTD simulation, the grid sizes in all three dimensions and the time step were chosen to be $\Delta x=\Delta y=\Delta z=\delta=0.5$ nm and $\Delta t=0.00095$ fs, respectively. In this case, the condition for convergence calculation, which is described as $c\Delta t \le \frac{1}{\sqrt{\frac{1}{(\Delta x)^2}+\frac{1}{(\Delta y)^2}+\frac{1}{(\Delta z)^2}}} = \frac{\delta}{\sqrt{3}}$ [33], is satisfied.

Basically, the optical force acting on a NP can be calculated by using the following formula [34]:

$$< \mathbf{F} >= \iint_S < \mathbf{T} > \cdot \mathbf{n} dS \quad (4)$$

where <T> is time-averaged Maxwell stress tensor and **n** is the normal of the surface enclosing the NP. In general, <T> can be expressed as follows [34]:

$$< \mathbf{T} >= \frac{1}{2}\text{Re}\left[\varepsilon \mathbf{E}\mathbf{E}^* + \frac{1}{\mu}\mathbf{B}\mathbf{B}^* - \frac{1}{2}\cdot\mathbf{I}\cdot\left(\varepsilon|\mathbf{E}|^2 + \frac{1}{\mu}|\mathbf{B}|^2\right)\right]. \quad (5)$$

Here, **E** and **B** represent the electric and magnetic fields on the surface and **I** is a unit tensor, ε and μ are the permittivity and permeability of the surrounding environment and they were chosen to be the values of water in this work which are $(8.85\times10^{-12})\times(1.33)^2$ F/m and $4\pi\times10^{-7}$ H/m, respectively.

In this paper, we calculated the electric and magnetic field distributions of the system by using the FDTD technique and the gradient forces acting on the NSs by using Eq. (4). Once the optical forces are obtained, the optical potential energies of NSs can be easily derived by using the following relationship:

$$< \mathbf{F}(r) >= -\nabla U(r). \quad (6)$$

Basically, the gradient force acting on a NP moving along the microfluid channel (i.e., the z direction) can be calculated by [27, 34]

$$< F_z(z) >= \frac{1}{2}\alpha' \frac{d}{dz}|E_z(0,0,z)|^2 \quad (7)$$

where α' is the real part of the polarizability of gold. This formula is valid for small particles (e.g., the Rayleigh particles considered in this paper) and E_z (0, 0, z) demotes the electric field at the center of the particle which is located at z. For particles in which the electric field is not uniform, we can use an averaged electric field intensity, which is defined as follows, as an approximation.

$$< |E_z(0,0,z)|^2 >= \frac{1}{V}\int_{\text{NS}} |E_z(x,y,z)|^2 dV \quad (8)$$

If the optical potential energy far from the antenna is set to be zero, then the optical potential energy of a NS at a position of z can be derived from the optical force $F_z(z)$ by using

$$U_z(z) = -\int_{-\infty}^{z} < F_z(z) > dz \quad (9)$$

By combining Eqs. (7), (8), and (9), one can easily obtain

$$U_z(z) = -\frac{1}{2V}\alpha' \int_{\text{NS}} |E_z(x,y,z)|^2 dV \quad (10)$$

Thus, the optical potential energy of a NS can be derived by Eq. (6) through the calculation of the optical force acting on the NS which can be done by using the FDTD technique. On the other hand, Eq. (10) indicates that the optical potential energy can also be obtained by directly calculating the integration of $|E|^2$ over the NS.

Results and Discussion

Trapping Au NSs of Different Sizes

When the antenna is excited with a focused fs laser light which is resonant with its LSPR, a strongly localized electric field with an enhancement factor as large as ~10^3–10^4 will be created in the gap region of the antenna [26]. As a result, a gradient force will be imposed on the NPs flowing in the channel, driving them toward the gap center. When a NP approaches the antenna, the localized electric field will be modified, leading to a redshift of the LSPR. Consequently,

the strong electric field is weakened in the constituent GNRs to some extent. It is apparent that the largest shift of the LSPR, which corresponds to the weakest electric field in the GNRs, is achieved when the NP is located at the gap center. In this case, the gradient force acting on the NP vanishes completely. It means that the bottom of the optical potential well is located at the gap center.

In our case, the optical forces acting on Au NSs are dominated by the gradient force which is induced by the strongly localized electric field in the gap of the antenna. Based on the FDTD technique, we can calculate the gradient forces for Au NSs with different diameters ranging from 3.0 to 5.0 nm. It should be emphasized that the optical force acting on a NS and the corresponding optical potential energy is proportional to the electric field or power density of the excitation light. For a power density of P=0.03 W/cm^2, we can readily derive the optical potential wells for Au NSs with different sizes by using Eq. (6), as shown in Fig. 3. It can be seen that the optical potential well becomes deeper for larger Au NSs and the depth of the optical potential well exceeds the kinetic energy of Brownian motion (k_BT), which is indicated by a dashed line in Fig. 3, for Au NSs with ϕ >3.0 nm. It implies that Au NSs with ϕ >3.0 nm can be stably trapped in the optical potential well when the power density of the excitation light exceeds 0.03 W/cm^2.

In order to estimate the sizes of NPs flowing in the channel, it is desirable that NPs can be trapped and released one by one. In Fig. 4, we present the dependence of the optical force on the position of the NS calculated for single and two Au NSs with ϕ=3.0 and 5.0 nm. For single Au NSs, it is found that the optical force increases gradually when the NS approaches the antenna. After reaching the maximum, it decreases rapidly and vanishes at the gap center of the antenna. The maximum optical force appears to be much larger for the NS with ϕ= 5.0 nm. Assuming that an Au NS with ϕ=3.0 nm has been

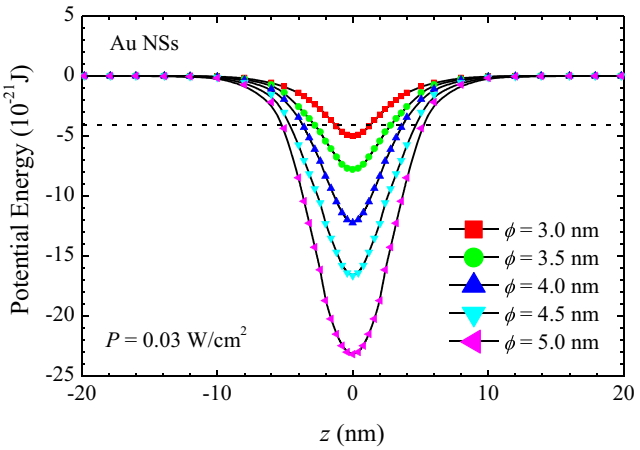

Fig. 3 Calculated optical potential wells formed in the gap of the antenna for Au NSs with different diameters at an excitation power density of P= 0.03 W/cm^2

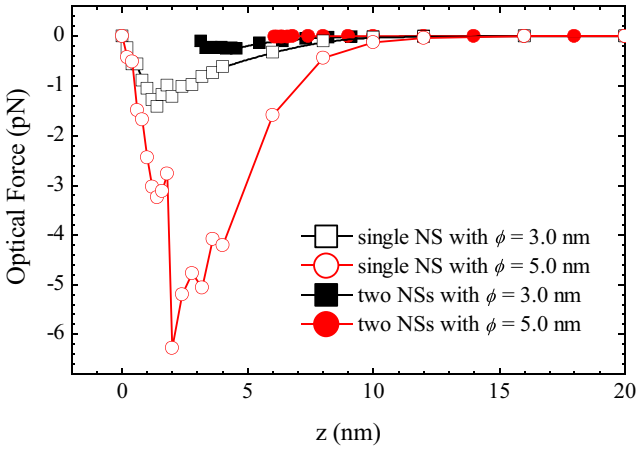

Fig. 4 Calculated optical forces imposed on Au NSs with ϕ=3.0 and 5.0 nm as a function of the locations of the Au NSs. The *empty squares* and *circles* denote the optical forces acting on the Au NSs by empty antenna. The *filled squares* and *circles* denote the optical forces acting on the second Au NS by the antenna with a trapped NS

stably trapped at the gap center of the antenna, we examined the optical force exerted on another Au NS with the same size near the antenna. As shown in Fig. 4, the optical force exerted on the second Au NS is reduced dramatically due to the existence of the first Au NS. Consequently, the possibility of trapping another Au NS is quite small because the optical potential energy in this case becomes much smaller than the kinetic energy of Brownian motion. For an Au NS with ϕ= 5.0 nm, a close inspection reveals that the optical force acting on the second NS almost disappears. Basically, this characteristic originates from the significant reduction of the local electric field caused by the trapped NS. In practical applications, this feature makes it possible to trap and release NPs one by one by designing an antenna with appropriate gap size. This is the basic condition for accurately measuring the sizes of NPs.

Modification in the TPL of the System by NSs of Different Sizes

Assuming that an Au NS is flowing in the channel, we can easily calculate the modification in the TPL of the system, which is expressed in terms of I_{NOR}, as a function of the position of the NS. It should be emphasized that one can only monitor the TPL of the whole system in practical devices. In some cases, the NS being detected may emit TPL when it is excited by the strong electric field generated by the antenna. However, we cannot discriminate the TPL emitted by the NS from that emitted by the antenna. For the NSs studied in this paper, Au NSs may emit TPL when they enter into the gap region of the antenna. In this case, we say that the Au NSs are lightened and they should be considered as a part of the antenna.

The dependence of the normalized TPL on the position of the NS calculated for Au NSs with different diameters ranging from 3.0 to 5.0 nm are presented in Fig. 5a. It is noticed that the modification in the TPL is quite sensitive to the sizes of Au NSs. For the small NS with ϕ=3.0 nm, the TPL begins to decrease at z~6 nm and the minimum I_{NOR} of ~0.82 is observed at the gap center. For the large NS with ϕ=5.0 nm, the modification of the TPL is observed at a longer distance of z~8 nm. In addition, the minimum I_{NOR} as small as ~0.08 is achieved. Based on the minimum I_{NOR} achieved at the gap center where the Au NS is stably trapped, one can easily obtain the information of the size of the Au NS. Moreover, the information on the optical potential energy of the Au NS at the gap center can also be derived by comparing Figs. 3 and 5a.

As mentioned above, an Au NS can be lightened when it approaches the antenna from a far place. Basically, the SPR of an Au NS appears at ~530 nm which is far from the LSPR of the antenna (~800 nm) [35]. Consequently, the electric field created in the Au NS is quite weak when it is excited at 800 nm. However, the situation is changed when it moves to the vicinity of the antenna. It is found that the electric field inside the NS becomes stronger and stronger when it approaches the antenna. In this case, the existence of the NS begins to influence the resonant frequency of the antenna and we should consider it as a part of the whole system. Different from practical experiments, we can easily extract the TPL of the Au NS and estimate the contribution of the NS to the total TPL in the numerical simulations. It is found that the TPL of the Au NS increases rapidly when it enters into the gap region and the maximum TPL is achieved when the Au NSs is trapped at the gap center.

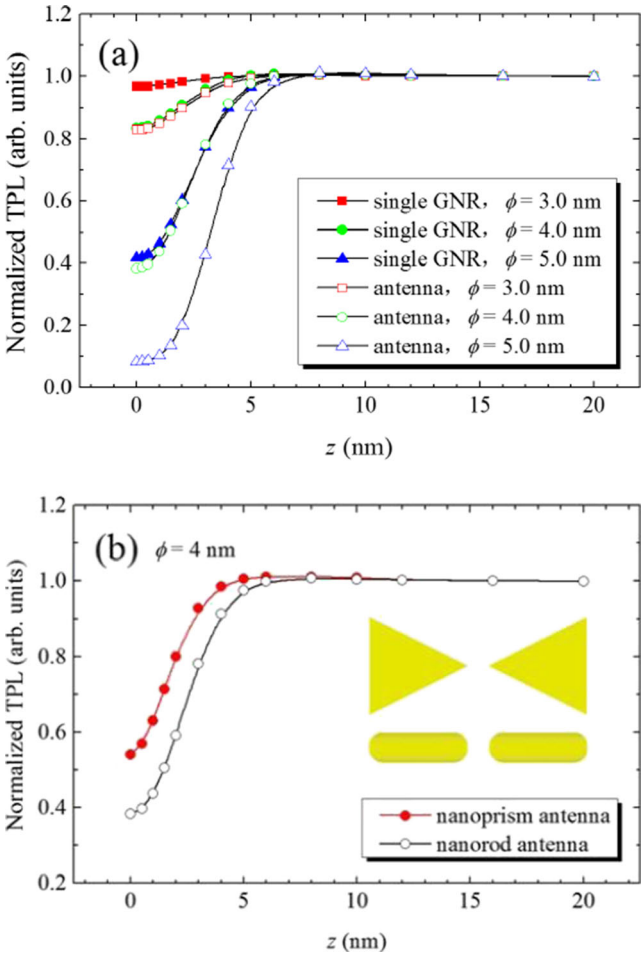

Fig. 5 **a** Dependence of the normalized TPL of the system (antenna+Au NS or single GNR+Au NS) on the location of the NS calculated for Au NSs with different diameters. **b** Dependence of the normalized TPL of the system on the location of the Au NS with ϕ=4.0 nm calculated for the nanorod-based antenna and the nanoprism-based antenna

Previously, we showed that the TPL emitted by single GNRs could be employed to detect NPs [7]. In order to show the effect of the significant enhancement in the electric field on the sensitivity of the antenna-based sensor, we compare the sensitivities of the two types of sensors in sensing Au NSs with ϕ=3.0, 4.0, and 5.0 nm, as shown in Fig. 5a. The sensor based on a single GNR was formed by removing a GNR from the antenna and the excitation wavelength was chosen at the LSPR of the single GNR (775 nm).

For the small Au NS with ϕ=3.0 nm, it can be seen that the minimum I_{NOR} obtained by the single-GNR-based sensor is only 0.96. In sharp contrast, the minimum I_{NOR} observed for the antenna-based sensor reaches 0.82. For the large Au NS with ϕ=5.0 nm, the minimum I_{NOR} achieved by the antenna-based sensor, which is only 0.08, is also much smaller than that obtained by the single-GNR-based sensor (0.41). Therefore, it clearly indicates that the sensors based on antennas possess much higher sensitivities than those built with single GNRs. It mainly originates from the significant enhancement in electric field in the gap region of the antenna.

We also compared the sensitivity of the nanorod-based antenna with that of a nanoprism-based antenna in the detection of an Au NS with ϕ=4.0 nm and the result is presented in Fig. 5b. The nanoprism-based antenna is composed of two nanoprisms with a side length of 25.5 nm and a thickness of 6 nm, as schematically shown in the inset of Fig. 5b. The excitation wavelength is chosen at the resonant wavelength of the nanoprism-based antenna (735 nm). In Fig. 5b, it can be seen that the minimum I_{NOR} achieved by the nanoprism-based antenna (~0.53) is larger than that achieved by the nanorod-based antenna (~0.39). In addition, the modification in TPL is observed at ~4.0 nm for the nanoprism-based antenna while it is observed at ~8.0 nm for the nanorod-based antenna. All these features indicate clearly that the sensitivity of the nanorod-based antenna is higher than that of the nanoprism-based one.

Apart from the detection of metallic NSs, the sensor we proposed may also be employed to detect NSs made of other materials. In Fig. 6a, we compare the dependence of I_{NOR} on the position of the NS for Au, Si, and SiO_2 NSs with the same diameter of ϕ=4.0 nm. For Si NSs, the evolution of the TPL

with decreasing distance appears to be similar to that observed for the Au NS because Si possesses a large refractive index. However, the minimum I_{NOR} observed at the gap center is larger than that observed for the Au NS. In addition, the distance at which the modification of the TPL occurs is smaller than that found for the Au NS. It implies that the sensitivity of the proposed sensor is lower for semiconductor NSs when comparing with metallic NSs. As compared with the Au and Si NSs, the modification in the TPL of the system induced by the SiO_2 NS is much smaller. In Fig. 6b, we present the relationship between the normalized TPL intensity at the gap center (z=0 nm) where the NS is stably trapped and the size of the NS calculated for Au, Si, and SiO_2 NSs. It should be emphasized that the Si NS may emit TPL and contribute to the TPL of the system. If the TPL emitted by the Si NS is much weaker than that of the antenna, then the I_{NOR} at the gap center can be used to estimate the size of the Si NS.

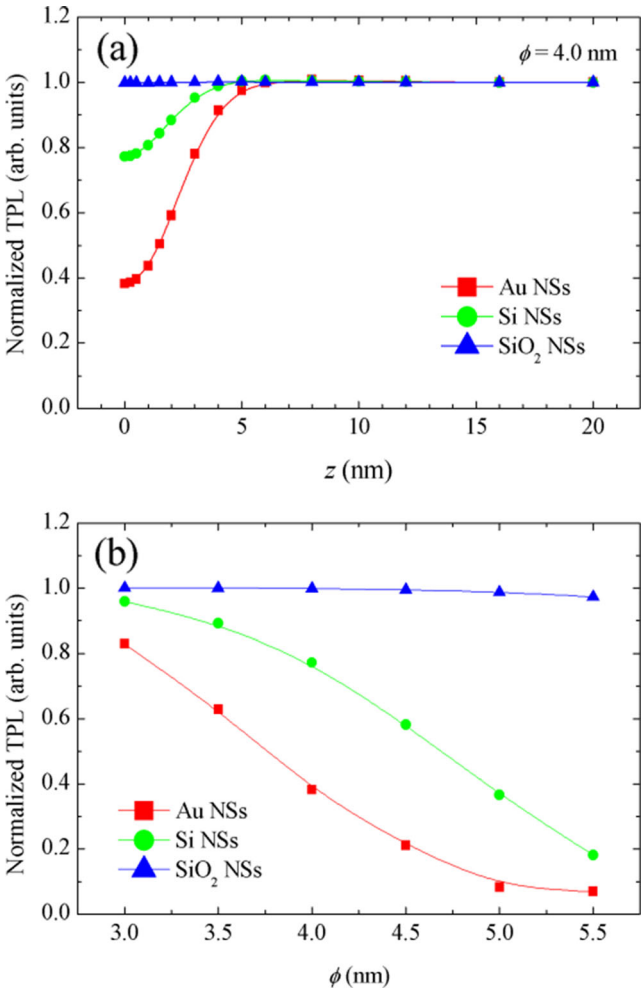

Fig. 6 **a** Dependence of the normalized TPL intensity of the system on the location of the NS calculated for Au, Si, and SiO_2 NSs with the same diameter of ϕ=4 nm. **b** Relationship between the normalized TPL intensity at the gap center (z=0 nm) and the size of the NS calculated for Au, Si, and SiO_2 NSs

Since the modification in local electric field is quite small for SiO_2 NSs of all sizes and for Si NSs with small sizes, the optical potential wells for these NSs are also very shallow as compared with Au NSs, implying the stable trapping of them will need much higher power densities. In addition, the small modification in the TPL of the system makes it difficult to accurately sense such NPs.

Relationship Between the TPL of the System and the Profile of the Optical Potential Energy

As mentioned above, a normalized TPL, which is expressed by Eq. (3), has been introduced to characterize the evolution of the TPL emitted by the system. In practice, the evolution of the TPL of the system during the trapping of a NS can be easily recorded. However, the information on the optical potential energy for the NS or the optical force acting on the NP is difficult to be obtained.

Based on the normalized TPL intensity of the system when an Au NS is stably trapped, one can easily derive the size of the Au NS, as shown in Fig. 6b. In addition, the optical potential energy of the Au NS at z=0 can also be deduced if the power density or the electric field of the fs laser light is known, as shown in Fig. 3. Therefore, a relationship between the optical potential energy of the Au NS at z=0 and the normalized TPL intensity can be easily established, as shown in Fig. 7. In other words, the optical potential energy of a NS at z=0 can be derived by measuring the normalized TPL of the system when the NS is stably trapped.

Apart from the optical potential energies of NSs at z=0, one can try to derive the profile of the optical potential energy for NSs moving in the microfluid channel. Basically, we have two ways to calculate the optical potential energy of a NS. The first method is to calculate the optical force acting on the NS and derive the optical potential energy according to Eq. (6). The second one is to calculate the integration of the electric field intensity over the NS based on Eq. (10). In Fig. 8, we compare the profiles of the optical potential energy obtained by using these two methods for Au NS with ϕ=4.0. The power density is chosen to be P=0.03 W/cm^2. In the second method, the real part of the polarizability of gold is the only parameter to be determined. If we make the optical potential energies at z=0 the same for the two cases, it can be seen that the two profiles coincide perfectly, verifying that the optical potential energy of a small NP can be deduced by calculating the integration of the electric field intensity over the NS.

In practical experiments, what we can directly measure is the normalized TPL intensity of the system. Therefore, we need to find out the relationship between the normalized TPL intensity of the system and that of the Au NS, which is an integration of $|\mathbf{E}|^4$ over the NS. When an Au NS approaches

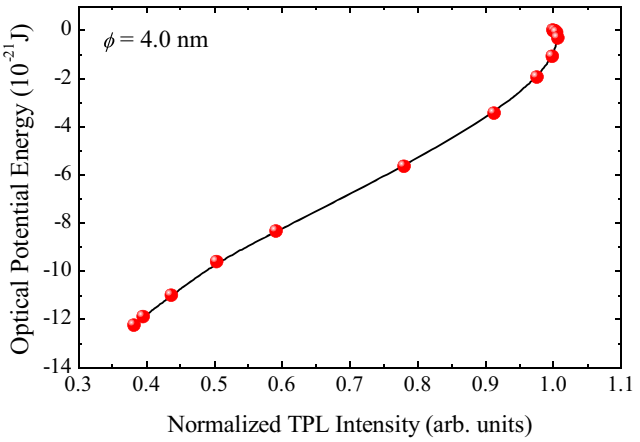

Fig. 7 Relationship between the optical potential energy and the normalized TPL intensity of the system at the gap center (z=0 nm) of the antenna calculated for the Au NS with ϕ=4.0 nm

the antenna from a far place, it is noticed that the NS is gradually lightened. This behavior is manifested in the TPL emitted by the NS which increases gradually at places far from the antenna and rapidly at places close to the antenna, as shown in the inset of Fig. 9. Although the TPL of the NS is much smaller than the total TPL of the system, it acts as a probe for the local electric field at the location of the NS. It is remarkable that the evolution of the TPL of the NS exhibits a profile quite similar to that of the TPL of the system except that the former is an increase of TPL while the latter is a decrease of TPL. In order to compare the two profiles, we change the sign for the TPL of the NS and intentionally make the TPL intensrities for the two profiles equal at z=0. As shown in Fig. 9, a perfect match between the profile for the TPL of the system and the transformed profile for the TPL of the NS is observed, indicating that the normalized TPL intensity of the system is closely related to the normalized TPL of the Au NS. It further confirms that the normalized TPL of the system, which is readily detected in practical experiments, can

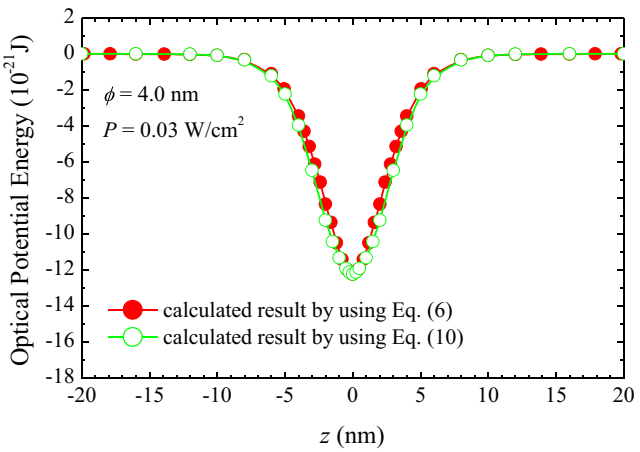

Fig. 8 Optical potential energy of a NS with ϕ=4.0 nm as a function of the position of the NS calculated by using Eqs. (6) and (10) which are based on the FDTD technique and the DDA method, respectively

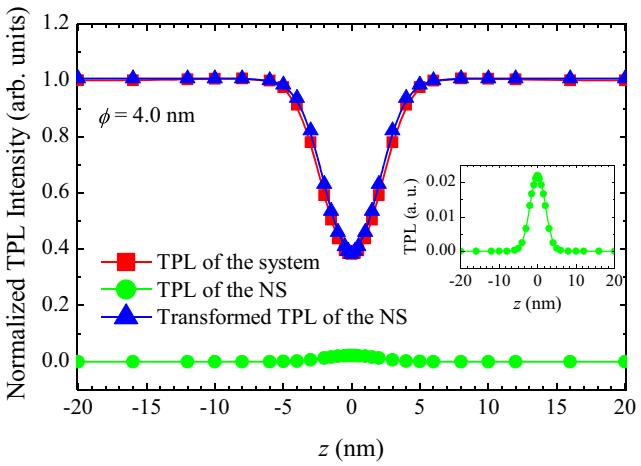

Fig. 9 Comparison of the normalized TPL intensity of the system and the transformed TPL intensity calculated for the Au NS with ϕ=4.0 nm. The normalized TPL intensity of the NS is also provided and magnified in the *inset*

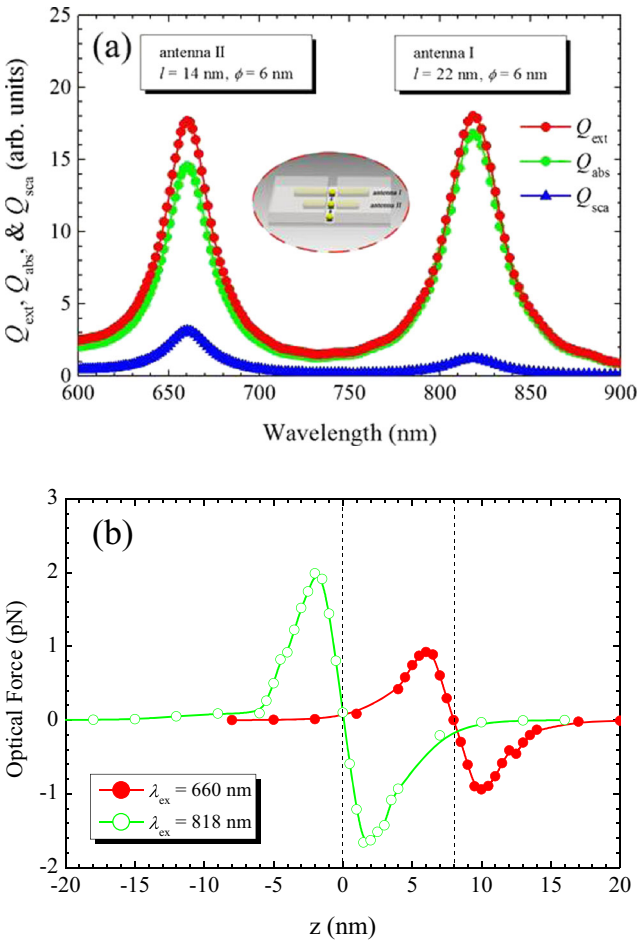

Fig. 10 **a** Calculated extinction, absorption, and scattering spectra of the sensor composed of two antennas arranged closely. **b** Position-dependent optical force acting on an Au NS with ϕ=3.0 nm calculated at the LSPRs of the two antennas. The gap centers of the two antennas are indicated by the *dashed lines*

be employed to derive the optical potential energy of the NS and thus the optical force acting on the NS. Once the profile of the normalized TPL intensity of the system is determined, the profile of the optical potential energy is given by the dependence of the square root of the normalized TPL intensity of the system on the position of the NS.

Trapping and Releasing NSs with Two Different Antennas Arranged Closely

As mentioned above, it is desirable to trap and release NPs flowing in the channel one by one. In order to realize such a function, we propose a device composed of two antennas arranged closely, as schematically shown in the inset of Fig. 10a. The sizes of the GNRs constituting the antennas are chosen to be 22 nm×6 nm and 14 nm×6 nm, respectively. The origin of the coordinate is chosen at the gap center of the large antenna (antenna I). The distance between the gap centers of the two antennas was set to be 8 nm. The extinction spectrum for the device is shown in Fig. 10a where two LSPRs corresponding to the two antennas are observed at 660 and 818 nm. We employed the FDTD technique to calculate the optical force acting on an Au NS with ϕ= 3.0 nm, and the result is presented in Fig. 10b for two excitation wavelengths which correspond to the LSPRs of the two antennas. In practice, the Au NS flowing in the channel is first trapped by the large antenna which is excited with fs laser light at 818 nm. When the wavelength of the trapping light is switched from 818 to 660 nm, the NS will be released by the large antenna and attracted to the center of the small antenna. In this way, one can realize the sequential trapping and releasing of NSs. In addition, the TPL emitted by the small antenna can be used to calibrate the information on the size of the NS estimated by the large antenna.

Summary

In summary, we proposed the use of a single antenna or two antennas to trap and sense NPs flowing in a microfluid channel. The sizes of NPs, which are eventually trapped at the gap center of the antenna, can be estimated by detecting the modification of the TPL of the system. It is shown that the sensitivity of the antenna-based sensors possess higher sensitivities than those built with single GNRs because of significantly enhanced electric field in the gap region. In addition, it is found that nanorod-based antennas are more sensitive than nanoprism-based antennas. The trapping probability for a second NP is significantly reduced for the antenna with a trapped NP, implying that trapping of NPs may occur sequentially. It is revealed that the detection of metallic NPs is much easier than that of semiconductor and dielectric NPs. In addition, the relationship between the evolution of TPL and the profile of optical potential well has been established. The sequential trapping and releasing of NPs flowing in the microfluid channel can be realized by designing a device composed of two antennas arranged closely. The results presented in this work clearly indicate that the significantly enhanced electric field created in the gap region of an antenna can be employed to trap NPs with small sizes sequentially and the modification in the TPL of the system can be utilized to extract the information on the sizes of NPs, the optical potential energy, and optical force.

Acknowledgments The authors acknowledge the financial support from the National Natural Science Foundation of China (Grant Nos. 51171066 and 11374109), the Ministry of Education of China (Grant No. 20114407110002), and the project for high-level professionals in the universities of Guangdong province, China. Q.-F. Dai would like to thank the Guangzhou science and technology project (Grant No. 2011J2200080).

References

1. Prasad PN (2004) Nanophotonics. John Wiley & Sons, New York
2. Mohamed MB, Volkov V, Link S, El-Sayed MA (2000) The 'lightning' gold nanorods: fluorescence enhancement of over a million compared to the gold metal. Chem Phys Lett 317:517–523
3. Chon JWM, Bullen C, Zijlstra P, Gu M (2007) Spectral encoding on gold nanorods doped in a silica sol-gel matrix and its application to high-density optical data storage. Adv Funct Mater 17:875–880
4. Zijlstra P, Chon JWM, Gu M (2009) Five-dimensional optical recording mediated by surface plasmons in gold nanorods. Nature 459: 410–413
5. Li X, Lan TH, Tien CH, Gu M (2012) Three-dimensional orientation-unlimited polarization encryption by a single optically configured vectorial beam. Nat Commun 3:998
6. Link S, Mohamed MB, El-Sayed MA (1999) Simulation of the optical absorption spectra of gold nanorods as a function of their aspect ratio and the effect of the medium dielectric constant. J Phys Chem B 103:3073–3077
7. Chen L, Li GC, Liu GY, Dai QF, Lan S, Tie SL, Deng HD (2013) Sensing the moving direction, position, size, and material type of nanoparticles with the two-photon-induced luminescence of a single gold nanorod. J Phys Chem C 117:20146–20153
8. Lu G, Hou L, Zhang T, Li W, Liu J, Perriat P, Gong Q (2011) Anisotropic plasmonic sensing of individual or coupled gold nanorods. J Phys Chem C 115:22877–22885
9. Zijlstra P, Paulo PMR, Orrit M (2012) Optical detection of single non-absorbing molecules using the surface plasmon resonance of a gold nanorod. Nat Nanotechnol 7:379–382
10. Shao L, Fang C, Chen H, Man YC, Wang J, Lin HQ (2012) Distinct plasmonic manifestation on gold nanorods induced by the spatial perturbation of small gold nanospheres. Nano Lett 12:1424–1430
11. Nie S, Emory SR (1997) Probing single molecules and single nanoparticles by surface-enhanced raman scattering. Science 275:1102–1106
12. Huang X, El-Sayed IH, Qian W, El-Sayed MA (2007) Cancer cells assemble and align gold nanorods conjugated to antibodies to produce highly enhanced, sharp, and polarized surface raman spectra: a potential cancer diagnostic marker. Nano Lett 7:1591–1597

13. Nikoobakht B, El-Sayed MA (2003) Surface-enhanced Raman scattering studies on aggregated gold nanorods. J Phys Chem A 107: 3372–3378
14. Bouhelier A, Bachelot R, Lerondel G, Kostcheev S, Royer P, Wiederrecht GP (2005) Surface plasmon characteristics of tunable photoluminescence in single gold nanorods. Phys Rev Lett 95: 267405
15. Qiu L, Larson TA, Smith D, Vitkin E, Modell MD (2008) Observation of plasmon line broadening in single gold nanorods. Appl Phys Lett 93:153106
16. Liu M, Pelton M, Guyot-Sionnest P (2009) Reduced damping of surface plasmons at low temperatures. Phys Rev B 79:035418
17. Deng HD, Li GC, Dai QF, Ouyang M, Lan S, Trofimov VA, Lysak TM (2013) Size dependent competition between second harmonic generation and two-photon luminescence observed in gold nanoparticles. Nanotechnology 24:075201
18. Ni W, Kou X, Yang Z, Wang J (2008) Tailoring longitudinal surface plasmon wavelengths, scattering and absorption cross sections of gold nanorods. ACS Nano 2:677–686
19. Ohlinger A, Deak A, Lutich AA, Feldmann J (2012) Optically trapped gold nanoparticle enables listening at the microscale. Phys Rev Lett 108:018101
20. Hubert C, Billot L, Adam PM, Bachelot R, Royer P, Grand J, Gindre D, Dorkenoo KD, Fort A (2008) Role of surface plasmon in second harmonic generation from gold nanorods. Appl Phys Lett 93:153106
21. Butet J, Thyagarajan K, Martin OJ (2013) Ultrasensitive optical shape characterization of gold nanoantennas using second harmonic generation. Nano Lett 13:1787–1792
22. Wang H, Huff TB, Zweifel DA, He W, Low PS, Wei A, Cheng J (2005) In vitro and in vivo two-photon luminescence imaging of single gold nanorods. Proc Natl Acad Sci U S A 102:15752–15756
23. Imura K, Nagahara T, Okamoto H (2005) Near-field two-photon-induced photoluminescence from single gold nanorods and imaging of plasmon modes. J Phys Chem B 109:13214–13220
24. Volpe G, Noack M, Aćimović SS, Reinhardt C, Quidant R (2012) Near-field mapping of plasmonic antennas by multiphoton absorption in poly (methyl methacrylate). Nano Lett 12:4864–4868
25. Schwartz O, Oron D (2009) Background-free third harmonic imaging of gold nanorods. Nano Lett 9:4093–4097
26. Mühlschlegel P, Eisler H-J, Martin OJF, Hecht B, Pohl DW (2005) Resonant optical antennas. Science 308:1607–1609
27. Zhang W, Huang L, Santschi C, Martin OJF (2010) Trapping and sensing 10 nm metal nanoparticles using plasmonic dipole antennas. Nano Lett 10:1006–1011
28. Juan ML, Righini M, Quidant R (2011) Plasmon nano-optical tweezers. Nat Photon 5:349–356
29. Yurkin MA, Hoekstra AG (2007) The discrete dipole approximation: an overview and recent developments. J Quant Spectro Ra 106:546–557
30. Draine BT, Flatau PJ (2010) User guide for the discrete dipole approximation code DDSCAT 7. 1. arXiv: 1002. 1505
31. Yee K (1966) Numerical solution of initial boundary value problems involving Maxwell's equations in isotropic media. IEEE Transactions on 14:302–307
32. Taflove A, Hagness SC (2005) Computational electrodynamics the finite-difference time-domain method, 3rd edn. Artech House, Boston, MA
33. Taflove A (1988) Review of the formulation and applications of the finite-difference time-domain method for numerical modeling of electromagnetic wave interactions with arbitrary structures. Wave Motion 10:547–582
34. Novotny L (2001) Forces in optical near-fields. In near-field optics and surface plasmon polaritons. Springer Berlin Heidelberg, Berlin, pp 123–141
35. Jain PK, Lee KS, El-Sayed IH, El-Sayed MA (2006) Calculated absorption and scattering properties of gold nanoparticles of different size, shape, and composition: applications in biological imaging and biomedicine. J Phys Chem B 110:7238–7248